

Evaluating Activity for Hydrogen-Evolving Cobalt and Nickel Complexes at Elevated Pressures of Hydrogen and Carbon Monoxide

Charles C. L. McCrory¹  · Nathaniel K. Szymczak¹ · Jonas C. Peters¹

Published online: 5 October 2015
© Springer Science+Business Media New York 2015

Abstract Molecular cobalt and nickel complexes are among the most promising homogeneous systems for electrocatalytic hydrogen evolution. However, there has been little exploration into the effect of gaseous co-additives such as CO and H₂, which may be present in operating hydrogen-evolving or carbon-dioxide reduction systems, on the performance of these molecular electrocatalysts. In this report, we investigate the electrocatalytic activity of six cobalt and nickel complexes supported by tetraazamacrocyclic or diazadiphosphacyclooctane ligands for the reduction of *p*-toluenesulfonic acid to hydrogen in acetonitrile under inert atmosphere and in the presence of CO and H₂. We present an elevated-pressure electrochemical apparatus capable of reaching CO and H₂ pressures of ca. 15–520 pounds per square inch (psia) (~1–35 atm), and we use this apparatus to determine binding constants for CO addition for each catalyst and study the inhibition of the electrocatalysis as a function of CO and H₂ pressure. In the case of CO, the extent of catalytic inhibition is correlated to the binding constant, with the cobalt complexes showing a greater degree of catalyst inhibition compared to the nickel complexes. In the case of H₂, no complex showed appreciable electrocatalytic inhibition even at H₂ pressures of ca. 500 psia.

Keywords Electrocatalysis · Hydrogen evolution · Water splitting · Solar fuels

Introduction

The electrocatalytic reduction of H⁺ to ½ H₂ by catalysts that incorporate inexpensive, earth-abundant materials is important to the development of solar-hydrogen production technologies [1–11]. Promising and extensively studied molecular electrocatalysts for hydrogen evolution include cobalt and nickel complexes supported by tetraazamacrocyclic or diazadiphosphacyclooctane ligands (Fig. 1) [12–32]. In particular, cobalt complexes 1–3 have been shown to catalyze electrochemical H₂ evolution from organic acids such as *p*-toluenesulfonic acid and various anilinium acids in CH₃CN [12–22]. The cobalt complex 4 was originally reported to evolve H₂ as a side reaction in electrocatalytic CO₂ reduction in CH₃CN [33, 34], and recently, efficient H₂ evolution by complex 4 and analogues of complex 2 have been reported under aqueous acidic (pH 2.2) conditions [23]. Additional systems of interest include the nickel complex 5 that has been shown to be active for H₂ evolution using HPF₆ in DMF and H₃PO₄ in aqueous solution [24] and the diazadiphosphacyclooctane nickel complex 6 which has been shown to catalyze H₂ evolution from various organic acids in CH₃CN [25–32].

A key point of interest for H₂-evolving catalysts is the effect of gaseous co-additives, which may be present at higher than atmospheric pressures, on the electrocatalytic efficiencies in the reaction system. For instance, an H₂-evolving system that functions to generate hydrogen on demand or to generate large quantities of hydrogen may require operating pressures that exceed 1 atm [35, 36]. Moreover, if an H₂-evolving system is to be coupled with a process for CO₂ (or CO) reduction, catalyst inhibition by such substrates must also be studied. In

Electronic supplementary material The online version of this article (doi:10.1007/s12678-015-0281-y) contains supplementary material, which is available to authorized users.

✉ Charles C. L. McCrory
cmccrory@umich.edu

✉ Jonas C. Peters
jpeters@caltech.edu

¹ Division of Chemistry and Chemical Engineering, California Institute of Technology, Pasadena, CA 91125, USA

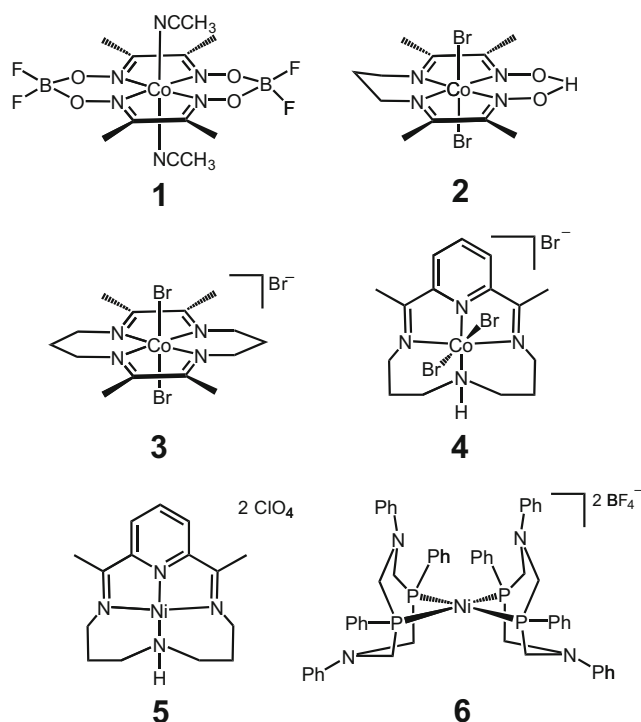


Fig. 1 Complexes investigated for electrocatalytic H₂ evolution

the case of hydrogenase enzymes, H₂ evolution by some [NiFe] hydrogenases is strongly inhibited by H₂ [37, 38], although this H₂ inhibition is not generally observed for [Fe-Fe] hydrogenases [39]. Reversible inhibition of electrocatalytic H₂ production by CO is reported for both [NiFe] and [FeFe] hydrogenases [37, 39–45]. Therefore, a reliable means to study electrocatalytic H₂-evolving efficiency as a function of pressures of H₂ and CO would be useful for the qualitative comparison of molecular biomimetic and nonbiomimetic functional hydrogenase systems.

Herein, the inhibition of electrocatalytic H₂ evolution at elevated pressures (ca. 500 pounds per square inch (psia)) of H₂ and CO was studied using a high-pressure electrochemical apparatus for molecular hydrogen-evolving catalysts **1–6** shown in Fig. 1. First, the electrocatalytic response of each complex under inert atmosphere for the reduction of *p*-toluenesulfonic acid (TsOH) in acetonitrile was analyzed using cyclic voltammetry and controlled-potential electrolysis. Subsequently, CO-binding constants were determined electrochemically for each complex, and the extent of catalytic inhibition by CO and H₂ was investigated at CO and H₂ pressures between ca. 15 and 520 psia. In general, the two nickel complexes **5–6** showed only modest attenuation of their electrocatalytic performance for H₂ evolution even at CO pressures of ca. 500 psia, whereas the electrocatalytic performance of cobalt complexes **1–4** all showed appreciable attenuation at CO pressures of only 15 psia (ca. 1 atm). None of the electrocatalysts investigated were appreciably inhibited by H₂ at any pressure up to ca. 500 psia.

Experimental

Materials According to literature procedures, **1** [46], **2** [47, 48], **3** [49, 50], **4** [51], **5** [52–55], and **6** [26, 56, 57] were prepared. Alphagaz HP-grade Ar (99.995 %) and Alphagaz 1-grade H₂ (99.999 %) were purchased from Air Liquide. Grade 4 (99.99 %) CO was purchased from Advanced Gas Technologies. CH₃CN, *p*-toluenesulfonic acid monohydrate (TsOH·H₂O), tetrafluoroboric acid etherate (HBF₄·Et₂O), hydrochloric acid etherate (HCl·Et₂O), triethylamine (Et₃N), and ferrocene were purchased from Sigma-Aldrich Co. and used as received. 2,6-Dichloroanilinium tetrafluoroborate (2,6-DCA) was prepared by the reaction between 2,6-dichloroaniline (Sigma Aldrich Co.) and HBF₄·Et₂O in diethyl ether, followed by washing the resulting solid with diethyl ether and drying in vacuo. Tetrabutylammonium perchlorate (*n*Bu₄NClO₄) was purchased from TCI America and recrystallized three times from ethanol. The amount of associated water in the recrystallized *n*Bu₄NClO₄ was determined to be ca. 0.02 mole fraction by ¹H-NMR integration of the residual water peak of vacuum-dried *n*Bu₄NClO₄ in CD₃CN.

Electrochemistry Electrochemical measurements were recorded with a CH Instruments 630-C Electrochemical Analyzer using the CHI Version 8.09 software package. For all electrochemical measurements, the electrolyte solution was 0.1 M *n*Bu₄NClO₄ in CH₃CN. The water concentration in a typical 0.1 M *n*Bu₄NClO₄ in CH₃CN electrolyte solution was independently determined by Karl Fischer coulometry using a Mettler-Toledo DL32 Karl Fischer Titrator with a Mettler-Toledo DM 143-SC double-pin platinum electrode and EMD Aquastar CombiCoulomat coulometric solvent. The water concentrations in four identical 0.1 M *n*Bu₄NClO₄ in CH₃CN solutions were measured, and the average was determined to be [H₂O]=0.035±0.004 M, which is the same as that measured for standard acetonitrile ([H₂O]=0.040±0.006 M).

Ambient pressure cyclic voltammetry (CV) measurements were conducted with a Pt wire auxiliary electrode and a Ag/AgNO₃ (1 mM)/CH₃CN nonaqueous reference electrode separated from the electrolyte solution by a Vycor frit (Bioanalytical Systems, Inc.). The working electrode was a 0.195 cm² glassy carbon rotating disk electrode (Pine Instrument Company). Each experiment was preceded by sparging the electrolyte solution for ca. 20 min with CH₃CN-saturated Ar, and measurements were recorded under a constant blanket of Ar. After each experiment, ferrocene was introduced to the electrolyte solution and the ferrocene/ferrocenium couple (Fc/Fc⁺=0.38 V vs. SCE) [58] was used to calibrate the reference electrode, and all potentials are reported versus the Fc/Fc⁺ couple. Unless otherwise indicated, all CV measurements were conducted at scan rates of 0.05 V/s.

Controlled-potential electrolysis experiments were conducted at ambient pressure in a sealed two-chamber cell where

the first chamber held the working and reference electrodes in 65 mL of 0.1 M $n\text{Bu}_4\text{NClO}_4$ in CH_3CN with 0.3 mM catalyst and 5.2 mM acid, and the second chamber held the auxiliary electrode in 25 mL of 0.1 M $n\text{Bu}_4\text{NClO}_4$ in CH_3CN . The two chambers were separated by a fine glass frit. The working and auxiliary electrodes were, 12 cm \times 3 cm \times 1 cm glassy carbon plates (Tokai Carbon, USA), and they were submerged such that ca. 64 cm 2 of each plate was in the electrolyte solution. The reference electrode was a Ag/AgNO $_3$ (1 mM)/ CH_3CN nonaqueous reference electrode separated from the solution by a Vycor frit (Bioanalytical Systems, Inc.). The cell was purged with N $_2$ for ca. 20 min and then sealed under an atmosphere of N $_2$ before the beginning of each controlled-potential electrolysis experiment. Each controlled-potential electrolysis experiment was conducted for 1 h at the specified potential under vigorous stirring, and the amount of H $_2$ evolved was quantified from an analysis of the headspace with an Agilent 7890A gas chromatograph using a thermal conductivity detector. The total amount of H $_2$ produced was determined as the sum of the H $_2$ in the headspace plus dissolved H $_2$ in the solution calculated using Henry's law, with a Henry's law constant $k_{\text{H}}=3.51\times 10^{-3}$ M atm $^{-1}$ [59]. Faradaic efficiencies were determined by dividing the measured H $_2$ produced by the amount of H $_2$ expected based on the charge passed during the controlled-potential electrolysis measurement.

High-pressure electrochemical measurements were conducted in a 5-L stainless steel Cortest Floor Autoclave Testing System rated at 3000 psig using a specially designed electrochemical cell (Fig. 2) similar to a previously reported system [60]. The autoclave pressure was measured with a pressure transducer and monitored with a Cortest Model 12.45 Pressure Vessel Control Panel. Pressure is reported here in absolute psia. The working electrode was a 0.078 cm 2 glassy carbon electrode (Bioanalytical Systems, Inc.), the auxiliary electrode was a Pt wire, and the reference electrode was a Ag/ $n\text{Bu}_4\text{NClO}_4$ (0.1 M)/ CH_3CN pseudo-reference electrode separated from the electrolyte solution by a Vycor frit. In each high-pressure electrochemical experiment, 0.15 mM ferrocene was included as an internal reference. Before each experiment, the sealed autoclave was purged with Ar for ca. 20 min. The autoclave was subsequently purged with H $_2$ or CO for ca. 20 min and then increased to the desired pressure of H $_2$ or CO and stirred for at least 5 min to allow for equilibration prior to each measurement.

Results and Discussion

Prior to conducting high-pressure measurements, cyclic voltammograms (CVs) of 0.3 mM solutions of each complex in 0.1 M $n\text{Bu}_4\text{NClO}_4$ in CH_3CN were measured, and the potentials for the M $^{3+/2+}$, M $^{2+/+}$, and M $^{+/0}$ redox couples are summarized in Table 1. The water concentration of the electrolyte

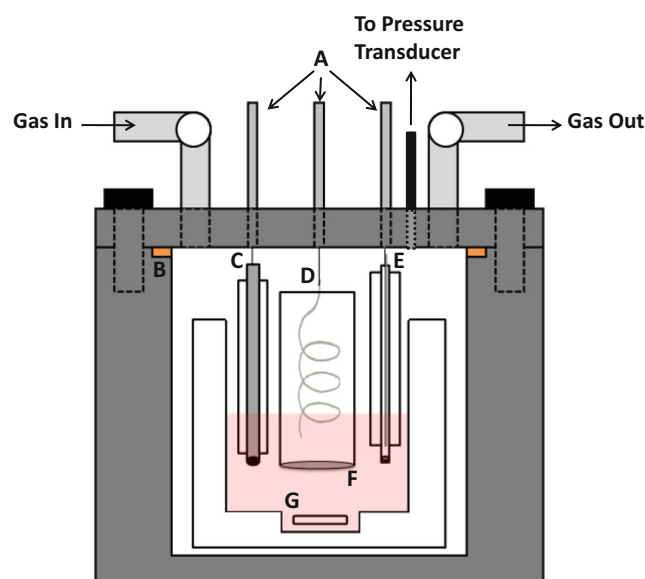


Fig. 2 High-pressure electrochemical system for electrocatalytic H $_2$ evolution under elevated H $_2$ and CO pressures. A glass electrochemical cell rests inside a modified stainless-steel autoclave. Electrical feedthrough (A), stainless steel gasket (B), glassy carbon working electrode (C), Pt auxiliary electrode (D), Ag/ CH_3CN pseudo-reference electrode separated from the electrolyte solution by a Vycor tip (E), fine glass frit separating auxiliary electrode from electrolyte solution (F), and stir bar (G)

solution was measured to be 35 ± 4 mM. Upon the addition of 5.2 mM TsOH \cdot H $_2$ O, there is an increase in the maximum reduction current that is consistent with electrocatalytic proton reduction (Fig. 3), and the reduction peak potentials, E_c , are summarized in Table 1. For complexes 1–3, E_c agrees with previously reported values for the reduction of TsOH \cdot H $_2$ O [16, 18]. Although we have previously reported electrolysis data for the electrocatalytic reduction of TsOH \cdot H $_2$ O by complex 4 [34], the electrocatalytic cyclic voltammograms and corresponding peak potentials have not been previously reported. Electrocatalytic TsOH \cdot H $_2$ O reduction in CH_3CN has not been previously reported for complexes 5 and 6.

To determine the Faradaic efficiency, ϵ , of each system, 1-h controlled-potential electrolyses were conducted at two potentials (–1.01 and –1.21 V) in stirred solutions of 0.3 mM catalyst and 5.2 mM TsOH \cdot H $_2$ O, and the headspaces above the solutions were sampled using gas chromatography after the electrolyses. This was used to determine the amount of H $_2$ evolved which was normalized for the charge passed in each electrolysis in order to determine ϵ . Each controlled-potential electrolysis and corresponding Faradaic efficiency determination was repeated at least three times for each catalyst investigated at both potentials. Note that for catalysts 3 and 4, the solution changes from the initial green color of the Co(III) precatalysts to red-purple upon electrolysis and returns to green upon exposure to air. These color changes are indicative of an electrochemical conversion of the Co(III) precatalyst to a more reduced resting state. For instance, in the case of complex 3, this change in color is consistent with

Table 1 Relevant parameters determined from cyclic voltammograms of 0.3 mM catalyst with and without 5.2 mM TsOH in CH₃CN (supporting electrolyte is 0.1 M (nBu₄N)ClO₄ in CH₃CN, scan rate=0.05 V/s) and 1-h controlled-potential electrolyses with 5.2 mM TsOH

Catalyst	$E_{M^{3+/2+}}^0$ (V)	$E_{M^{2+/+}}^0$ (V)	$E_{M^{+/0}}^0$ (V)	E_c (V)	-1.01 V		-1.21 V	
					q (C)	ε (%)	q (C)	ε (%)
1	–	-0.92 ^{a,b}	–	-0.98 ^{a,c}	14±1	93±4	20±5	85±10
2	-0.52 ^c	-1.10 ^c	–	-0.87 ^c	10±2	53±5	16±3	50±5
3	-0.43 ^a	-0.75 ^a	–	-0.80 ^a	7±2	80±5	9±2	73±4
4	-0.41	-0.92	–	-0.99	8±1 ^f	87±4 ^f	12±3 ^f	86±8 ^f
5	0.92 ^d	-1.02 ^d	-1.63 ^d	-0.90	3.0±0.4	42±16	14±2	71±8
6	–	-0.85 ^e	-1.03 ^e	-0.89	11±3	95±2	16±2	90±6

All tabulated potentials were measured in this study, but some values of E^0 and E_c have been previously reported. Complexes **3** and **5** show two catalytic waves, and only measurements from the more positive catalytic peak are tabulated.

^a [16]

^b [17]

^c [18]

^d [55]

^e [26]

^f The CPE data for complex **4** shown here has been previously reported in [34]

the reduction of the precatalyst to its Co(II) state under electrolysis conditions [16, 61]. The charge passed during the 1-h controlled-potential electrolyses and corresponding ε for each catalyst at -1.01 V and -1.21 V for the reduction of TsOH·H₂O are reported with standard deviations in Table 1. Note that we have previously reported the controlled-potential electrolysis data by complex **4** [34] and include that data here for completeness.

Complexes **1**, **4**, and **6** catalyze TsOH·H₂O reduction with ε =ca. 90 % which agrees with previous studies for **1** [15–17]. In contrast, **2** operates with ε =ca. 50 % for TsOH·H₂O reduction under these conditions as previously reported [18]. The low ε for **2** may be caused by the turnover-dependent degradation of the catalyst. Such degradation has been reported for similar cobalt tetraamine complexes in neutral and alkaline aqueous solutions at mercury [62, 63] and FTO [64] electrodes or in acetonitrile in the presence of wet strong acids and electrolytes at carbon electrodes [65]. This hypothesis regarding catalyst decomposition is further supported by the deviation from linearity of charge-time plots from the controlled-potential electrolysis measurements (Fig. S1). If one assumes that the 47 % of total charge passed in the electrolysis of **2** and TsOH·H₂O not related to H₂ formation is instead due to catalyst decomposition, then this would be consistent with the four-electron reduction of ca. two thirds of the catalyst molecules present in the electrolysis solution. Note that in the presence of 2,6-DCA (pK_a=5.1) as the acid source [66], **2** operates with ε =ca. 98 % at -1.01 V (Fig. S1). This suggests that the proposed catalyst degradation of **2** in TsOH·H₂O may not be general but, instead, depends on the acid source. Catalyst **3** operates with ε =ca. 80 %, which is close

to the previously reported Faradaic efficiency ε =90 % for the reduction of 21 mM TsOH·H₂O by 0.9 mM **3** [16]. The large standard deviation for the Faradaic efficiency of **5** at -1.01 V may be attributed to the large error inherent in measuring the small amounts of H₂ generated due to low catalyst activity for **5** at this potential. At -1.21 V, the electrolysis measurement with **5** results in more charge passed, allowing for a more precise measurement of ε =ca. 70 %.

The inhibition of each of these catalytic systems by elevated pressures of CO (a common poison for Co and Ni catalysts) and H₂ (the electrocatalytic product) was investigated at pressures ranging from ca. 14 to 520 psia using a specially designed high-pressure electrochemical apparatus (Fig. 2). Upon exposing each catalyst to elevated pressures of CO in CH₃CN in the absence of acid, there is a positive shift of E^0 for the Co^{2+/+} or Ni^{2+/+} redox couple with increasing CO pressure (Fig. 4). The observed positive shift is indicative of CO coordination to the M⁺ complex (Scheme 1).

It is possible to determine the CO-binding equilibrium constant, K_{CO} , for each system from this shift in $E_{M^{2+/+}}$ as a function of CO pressure as shown in Eq. 1 [67–71].

$$E - E_{M^{2+/+}}^0 = \frac{RT}{nF} \ln(1 + [\text{CO}]K_{CO}) \quad (1)$$

Here, E is the measured potential, R is the ideal gas constant, T =298 K is the temperature, n =1 is the number of electrons during the redox process, F is Faraday's constant, $[\text{CO}]$ is the concentration of CO in solution calculated from Henry's law using the Henry's law constant k_H =8.3×10⁻³ M atm⁻¹ [71], and K_{CO} is the CO-

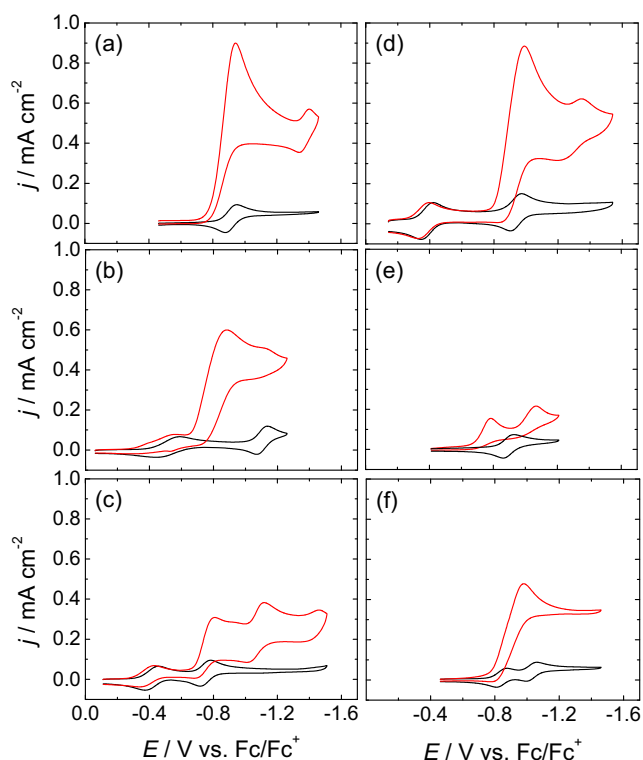


Fig. 3 Cyclic voltammograms in solutions of 0.3 mM **a 1**, **b 2**, **c 3**, **d 4**, **e 5**, and **f 6** with no acid (*black*) and in the presence of 5.2 mM TsOH·H₂O (*red*) (supporting electrolyte is 0.1 M *n*Bu₄NClO₄ in CH₃CN, scan rate=0.05 V/s)

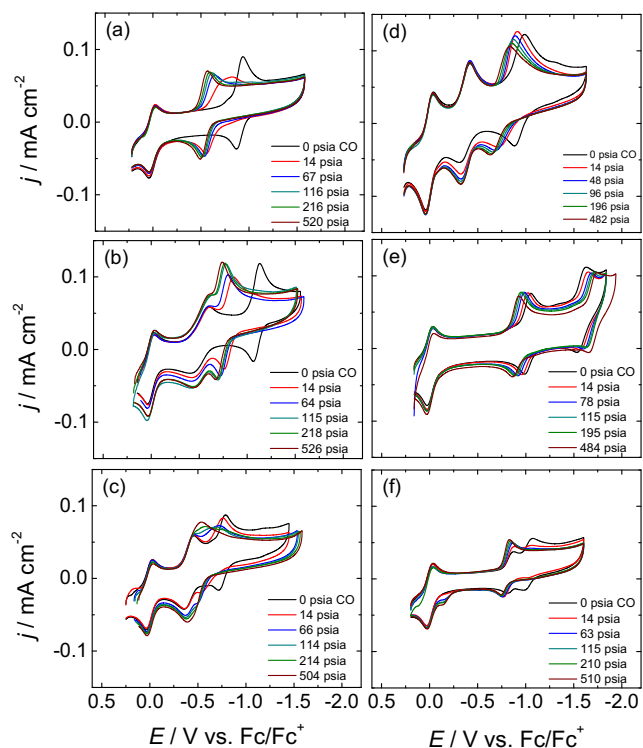
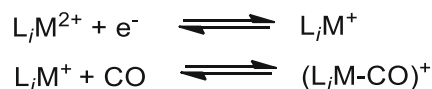


Fig. 4 Cyclic voltammograms at varying pressures of CO with 0.15 mM ferrocene and 0.3 mM **a 1**, **b 2**, **c 3**, **d 4**, **e 5**, and **f 6** (supporting electrolyte is 0.1 M *n*Bu₄NClO₄ in CH₃CN, scan rate=0.05 V/s)



Scheme 1 Proposed mechanism of CO binding for a generic complex $L_i M^{2+}$

binding equilibrium constant and given by Eq. 2.

$$K_{CO} = \frac{[(L_i M-CO)^+]}{[L_i M^{m+1}][CO]} \quad (2)$$

A plot of $(E - E_{M^{2+/+}}^0)$ as a function of [CO] for each catalyst is shown in Fig. 5. Fitting the reported data by Eq. 1 using the Levenberg-Marquardt algorithm yields the following: $K_{CO}(1) = (6.5 \pm 0.8) \times 10^6 \text{ M}^{-1}$, $K_{CO}(2) = (1.1 \pm 0.2) \times 10^7 \text{ M}^{-1}$, $K_{CO}(3) = (3.5 \pm 0.9) \times 10^4 \text{ M}^{-1}$, $K_{CO}(4) = (1.0 \pm 0.1) \times 10^5 \text{ M}^{-1}$, $K_{CO}(5) = (5.6 \pm 0.4) \times 10^2 \text{ M}^{-1}$, and $K_{CO}(6) = (4.3 \pm 0.4) \times 10^2 \text{ M}^{-1}$. Note that the K_{CO} for complex **3** measured in this study matches well with the value determined in a previous study [71]. Also, the comparatively small binding constants for **5** and **6** are consistent with a previous study reporting that reduced forms of complex **6** do not coordinate CO at 1 atm (ca. 15 psia) [72], suggesting that high pressures of CO are necessary to measure the binding constants of these complexes that coordinate CO weakly such as complexes **5** and **6**.

To study inhibition of electrocatalytic H₂ evolution by CO, CVs of 0.3 mM catalyst in the presence of 5.2 mM TsOH·H₂O were measured at varying pressures of CO (Fig. 6a–f). Electrocatalytic H₂ evolution is inhibited by CO for each catalyst. The extent of inhibition for each catalyst can be better illustrated by a plot of the fraction of the measured peak current at each CO pressure (j_{CO}) divided by the initial peak current in the

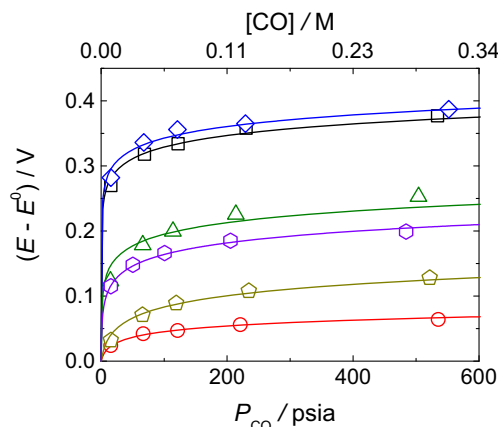
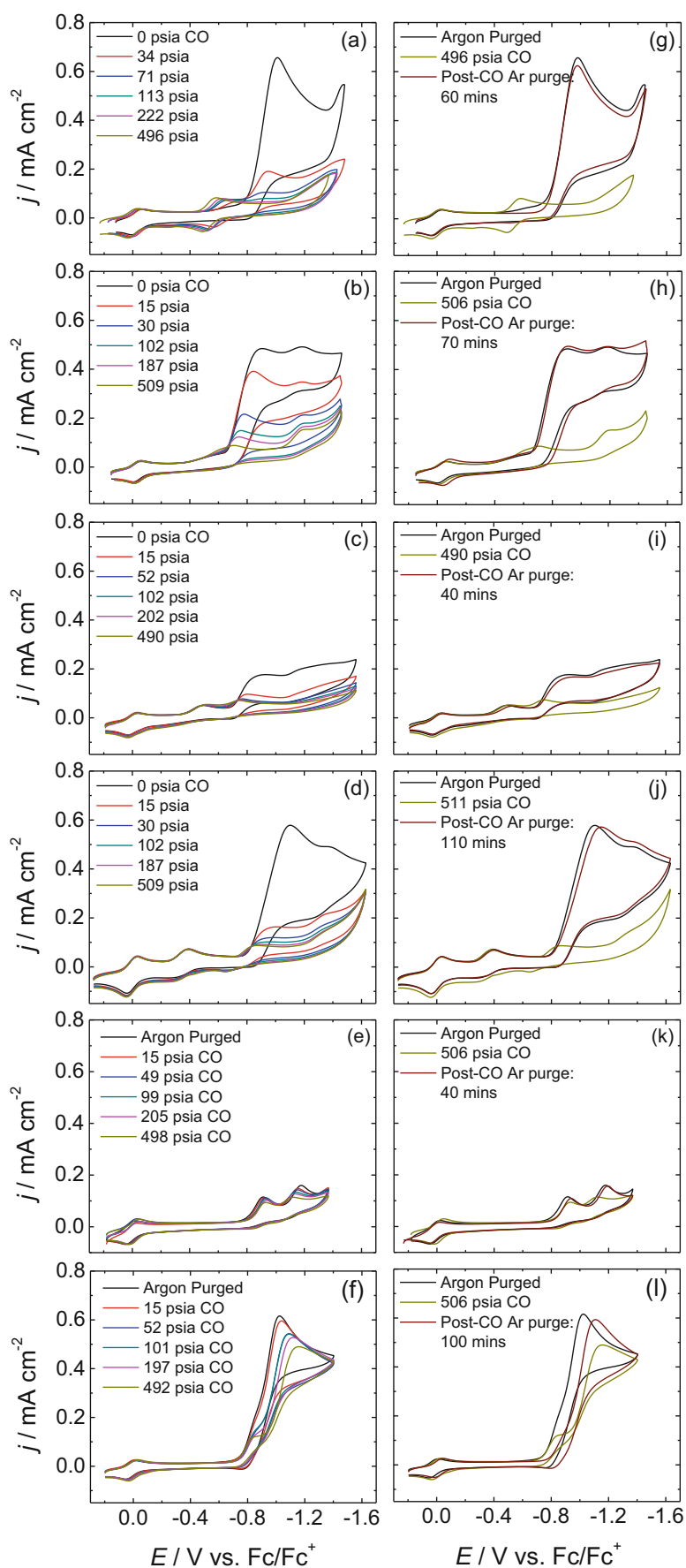


Fig. 5 Anodic potential shift from standard redox potential at elevated CO pressure for **1** (*black squares*), **2** (*blue diamonds*), **3** (*green triangles*), **4** (*purple hexagons*), **5** (*yellow pentagons*), and **6** (*red circles*). The *solid lines* are fits to each data set by Eq. 1

Fig. 6 a–f Cyclic voltammograms of 5.2 mM TsOH·H₂O with 0.15 mM ferrocene and 0.3 mM **a 1**, **b 2**, **c 3**, **d 4**, **e 5**, and **f 6**, g–l Cyclic voltammograms of **g 1**, **h 2**, **i 3**, **j 4**, **k 5**, and **l 6** under the same conditions as a–f but measured before exposure to CO, at ca. 500 psia CO, and after purging the same system with Ar (supporting electrolyte is 0.1 M *n*Bu₄NClO₄ in CH₃CN, scan rate=0.05 V/s)



absence of CO (j_c) as seen in Fig. 7. From this data, it is clear that there is a stronger CO inhibition of H₂ evolution catalyzed by the cobalt complexes **1–4** compared to the nickel complexes **5** and **6**. After being exposed to ca. 500 psia CO, each catalyst system was purged with Ar for ca. 60–120 min and reinvestigated for electrocatalytic H₂ evolution by cyclic voltammetry (Fig. 6g–l). The resulting cyclic voltammograms are equivalent to those measured before exposure to CO for **1–5**, suggesting reversible CO inhibition. In the case of **6**, the voltammogram measured after CO exposure has the same peak current as the pre-exposure voltammogram, but the peak potential is shifted ca. 0.1 V negative.

The inhibition of electrocatalytic H₂ evolution by elevated pressures of CO likely occurs via the formation of a stable CO adduct (Scheme 1) that competes with catalyst protonation. The extent of the CO inhibition for each catalyst is therefore dependent on its relative CO- and H⁺-binding affinities. This is supported by the reported measurements of K_{CO} . Complexes **1** and **4**, which have the largest determined K_{CO} , also show the greatest extent of CO inhibition. However, **5** and **6**, whose CO-binding affinities are ca. 5 orders of magnitude less than **1** and **2**, show much less inhibition by CO. Note that although $K_{CO(2)} > K_{CO(1)}$, H₂ evolution by **1** is more inhibited by CO than is **2**. This suggests that the proton-binding affinity of **2** is likely greater than that of **1**.

Interestingly, we have recently reported that cobalt complex **4** shows reasonably high activity and selectivity for CO₂ reduction to CO in CH₃CN with 10 M water as the

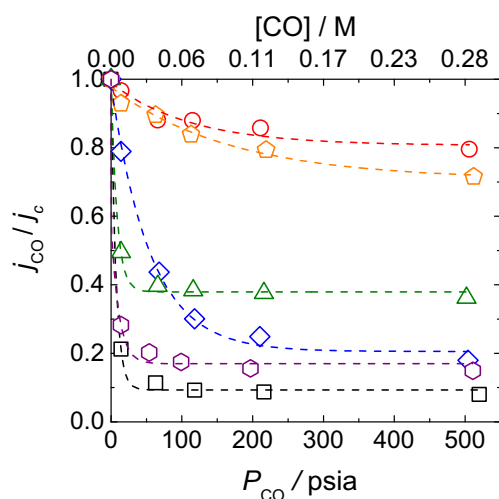


Fig. 7 Fraction of the electrocatalytic TsOH reduction current retained upon exposure to varying pressures of CO for **1** (black squares), **2** (blue diamonds), **3** (green triangles), **4** (purple hexagons), **5** (orange pentagons), and **6** (red circles). The dashed lines are guides to the eye and not indicative of actual fits to the data.

acid source [34]. The selectivity for CO₂ reduction over H₂ evolution by **4** in this previous study may be due to selective inhibition of the H₂ evolution kinetics due to reversible coordination of electrochemically generated CO, leading to a preferential reduction of CO₂.

Our lab has previously reported that **1** qualitatively retains its ability to mediate electrocatalytic H₂ evolution to an appreciable extent even under an atmosphere of CO in sufficiently acidic solutions [14]. However, our high-pressure studies suggest that **1** is significantly inhibited by CO at even moderate CO pressures. In light of this, experiments were conducted with four acids with varying pK_a s under an atmosphere of CO: tetrafluoroboric acid etherate (HBF₄·Et₂O, $pK_a=0.1$) [73], 2,6-DCA ($pK_a=5.1$) [66], TsOH·H₂O ($pK_a=8$) [73], and hydrochloric acid etherate (HCl·Et₂O, $pK_a=8.9$) [73]. An atmosphere of CO was achieved by sparging Ar-purged electrolyte solutions with CO for ca. 10 min and then blanketing the solutions with CO during the course of the electrochemical measurements. CVs of electrocatalytic H₂ evolution by **1** in CO-sparged solutions for each acid are shown in Fig. 8. The electrocatalytic H₂ evolution by **1** is inhibited by an atmosphere of CO even in the presence of strong acids such as HBF₄·Et₂O. However, inhibition of the electrocatalytic H₂ evolution by CO is slightly greater when weaker acids are used: $j_{CO}/j_c=0.55$ for HBF₄·Et₂O, $j_{CO}/j_c=0.61$ for 2,6-DCA, $j_{CO}/j_c=0.25$ for TsOH·H₂O, and $j_{CO}/j_c=0.18$ for HCl·Et₂O.

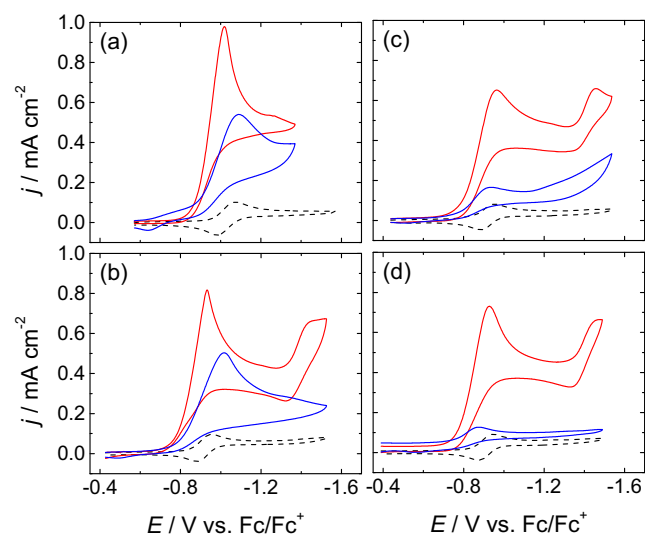


Fig. 8 Cyclic voltammogram of the electrocatalytic H₂ evolution by **1** with **a** HBF₄·Et₂O, **b** 2,6-DCA, **c** TsOH·H₂O, and **d** HCl·Et₂O as the acid source. The dashed black line is 0.3 mM **1** in the absence of acid and the solid red line 0.3 mM **1** with 5.2 mM acid, and the solid blue line is 0.3 mM **1** with 5.2 mM acid under an atmosphere of CO (supporting electrolyte is 0.1 M *n*Bu₄NClO₄ in CH₃CN, scan rate=0.05 V/s)

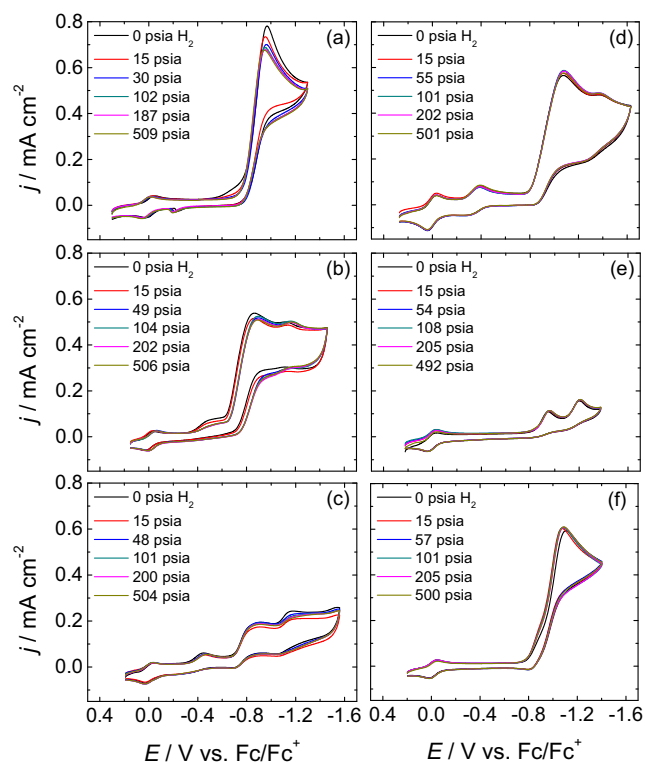


Fig. 9 Cyclic voltammograms of 5.2 mM TsOH·H₂O with 0.15 mM ferrocene and 0.3 mM **a 1**, **b 2**, **c 3**, **d 4**, **e 5**, and **f 6** (supporting electrolyte is 0.1 M *n*Bu₄NClO₄ in CH₃CN, scan rate=0.05 V/s)

Electrocatalytic H₂ evolution by each complex in the presence of elevated pressures of H₂ was also investigated, and CVs of each catalyst in the presence of TsOH·H₂O at varying pressures of H₂ failed to show measurable inhibition for any of the catalysts (Fig. 9). The lack of inhibition by H₂ suggests that H₂ does not bind strongly to the reduced catalyst species and may also be consistent with the notion that the elimination of H₂ is subsequent to the rate-limiting step in the H₂ evolution mechanism [12–21, 25–32, 74–78]. For 1–3, the catalytic cycle is thought to operate via an initial rate-limiting protonation of the Co^I complex to form a Co^{III}-H species [12–21, 74–78], which is consistent with the lack of observed inhibition by H₂. In contrast, the proposed mechanism of **6** is thought to operate with either rate-limiting H₂ elimination or an intramolecular proton transfer [25–32]. The lack of observed H₂ inhibition may support the latter as the primary rate-limiting step. In addition, because catalyst **5** has been previously shown to reversibly coordinate H₂ under basic conditions and elevated pressures of H₂ [26, 30], its electrochemical behavior was investigated under high pressures

of H₂ and basic conditions. However, no electrocatalytic H₂ oxidation was observed in the presence of ca. 800 equivalents Et₃N even at 523 psia H₂ (Fig. S2).

It is interesting to compare the response of these molecular hydrogen-evolving catalysts to H₂ and CO with the hydrogenase enzymes. In particular, the general lack of product inhibition of H₂ evolution by the molecular catalysts investigated is markedly different than the behavior of the [NiFe] hydrogenases for which full inhibition of H₂ production at 1 atm H₂ is reported [37, 45]. However, each synthetic catalyst showed varying degrees of reversible CO inhibition, and each was at least partially inhibited at 1 atm of CO. This is similar to the reported behavior for both [NiFe] and [FeFe] hydrogenase enzymes, which show partial inhibition for H₂ production at 1 atm (ca. 15 psia) CO [37, 39–45].

Conclusions

We have presented a high-pressure electrochemical apparatus for investigating electrocatalytic H₂ evolution with molecular catalysts under elevated pressures of H₂ and CO relevant to a hydrogen production and storage device [35, 36]. It was shown that CO inhibited H₂ evolution rates in all cases, likely through the formation of stable CO adducts, and the extent of the inhibition depends on the CO- and H⁺-binding affinities for each complex. In general, the Ni complexes **5** and **6** showed a lower affinity for CO coordination compared to the Co complexes **1–4** and therefore were comparatively less inhibited for H₂ evolution. Each of the Co complexes **1–4** showed appreciable attenuation of their electrocatalytic response by only 15 psia (ca. 1 atm) of CO, although the extent of the inhibition is also dependent on the acid source used in the case of H₂ evolution by complex. Of particular interest is the inhibition of H₂ evolution for complex **4** by CO—the previously reported selectivity of complex **4** for CO₂ reduction over H₂ evolution may be due to preferential inhibition of H₂ evolution reaction by coordination of electrochemically generated CO. This suggests that CO-binding affinities may be useful indicators for the relative selectivity of CO₂ reduction catalysts for CO₂ reduction over competitive H₂ evolution. In contrast to the CO inhibition studies, there was no evidence of electrocatalytic inhibition of H₂ evolution at elevated pressures of H₂. This latter result suggests that H₂ elimination is likely not a rate-limiting step in the H₂ evolution mechanism for catalysts **1–6** under the conditions reported here.

Acknowledgments Financial support for this work was provided by an NSF Center for Chemical Innovation (CHE-0802907). We also thank David C. Lacy and Wesley K. Kramer for many useful discussions.

References

- M. Grätzel, *Acc. Chem. Res.* **14**, 376–384 (1981)
- U. Koelle, *New J. Chem.* **16**, 157–169 (1992)
- A.J. Bard, M.A. Fox, *Acc. Chem. Res.* **28**, 141–145 (1995)
- J.A. Turner, *Science* **305**, 972–974 (2004)
- V. Artero, M. Fontecave, *Coord. Chem. Rev.* **249**, 1518–1535 (2005)
- N.S. Lewis, D.G. Nocera, *Proc. Natl. Acad. Sci.* **103**, 15729–15735 (2006)
- N.S. Lewis, *Science* **315**, 798–801 (2007)
- G.W. Crabtree, M.S. Dresselhaus, *MRS Bull.* **33**, 421–428 (2008)
- H.B. Gray, *Nat. Chem.* **1**, 7 (2009)
- T.R. Cook, D.K. Dogutan, S.Y. Reece, Y. Surendranath, T.S. Teets, D.G. Nocera, *Chem. Rev.* **110**, 6474–6502 (2010)
- M.G. Walter, E.L. Warren, J.R. McKone, S.W. Boettcher, Q. Mi, E.A. Santori, N.S. Lewis, *Chem. Rev.* **110**, 6446–6473 (2010)
- T.-H. Chao, J.H. Espenson, *J. Am. Chem. Soc.* **100**, 129–133 (1978)
- P. Connolly, J.H. Espenson, *Inorg. Chem.* **25**, 2684–2688 (1986)
- X. Hu, B. M. Cossairt, B. S. Brunenschwig, N. S. Lewis, J. C. Peters, *Chem. Commun.*, 4723–4725 (2005)
- M. Razavet, V. Artero, M. Fontecave, *Inorg. Chem.* **44**, 4786–4795 (2005)
- X. Hu, B.S. Brunenschwig, J.C. Peters, *J. Am. Chem. Soc.* **129**, 8988–8998 (2007)
- C. Baffert, V. Artero, M. Fontecave, *Inorg. Chem.* **46**, 1817–1824 (2007)
- P.-A. Jacques, V. Artero, J. Pecaut, M. Fontecave, *Proc. Natl. Acad. Sci.* **106**, 20627–20632 (2009)
- J.L. Dempsey, B.S. Brunenschwig, J.R. Winkler, H.B. Gray, *Acc. Chem. Res.* **42**, 1995–2004 (2009)
- V. Fourmond, P.-A. Jacques, M. Fontecave, V. Artero, *Inorg. Chem.* **49**, 10338–10347 (2010)
- S. Losse, J.G. Vos, S. Rau, *Coord. Chem. Rev.* **254**, 2492–2504 (2010)
- N. Kaefter, M. Chavarot-Kerlidou, V. Artero, *Acc. Chem. Res.* (2015)
- C.C.L. McCrory, C. Uyeda, J.C. Peters, *J. Am. Chem. Soc.* **134**, 3164–3170 (2012)
- L.L. Efros, H.H. Thorp, G.W. Brudvig, R.H. Crabtree, *Inorg. Chem.* **31**, 1722–1724 (1992)
- C.J. Curtis, A. Miedaner, R. Ciancanelli, W.W. Ellis, B.C. Noll, M. Rakowski DuBois, D.L. DuBois, *Inorg. Chem.* **42**, 216–227 (2002)
- A.D. Wilson, R.H. Newell, M.J. McNevin, J.T. Muckerman, M. Rakowski DuBois, D.L. DuBois, *J. Am. Chem. Soc.* **128**, 358–366 (2005)
- A.D. Wilson, R.K. Shoemaker, A. Miedaner, J.T. Muckerman, D.L. DuBois, M.R. DuBois, *Proc. Natl. Acad. Sci.* **104**, 6951–6956 (2007)
- M.R. DuBois, D.L. DuBois, *Comptes Rendus Chimie* **11**, 805–817 (2008)
- M.R. DuBois, D.L. DuBois, *Acc. Chem. Res.* **42**, 1974–1982 (2009)
- M.R. DuBois, D.L. DuBois, *Chem. Soc. Rev.* **38**, 62–72 (2009)
- A. Le Goff, V. Artero, B. Jusselme, P.D. Tran, N. Guillet, R. Metaye, A. Fihri, S. Palacin, M. Fontecave, *Science* **326**, 1384–1387 (2009)
- U.J. Kilgore, J.A.S. Roberts, D.H. Pool, A.M. Appel, M.P. Stewart, M.R. DuBois, W.G. Dougherty, W.S. Kassel, R.M. Bullock, D.L. DuBois, *J. Am. Chem. Soc.* **133**, 5861–5872 (2011)
- A.H.A. Tinnemans, T.P.M. Koster, D.H.M.W. Thewissen, A. Mackor, *Recl. Trav. Chim. Pay. B.* **103**, 288–295 (1984)
- D.C. Lacy, C.C.L. McCrory, J.C. Peters, *Inorg. Chem.* **53**, 4980–4988 (2014)
- Targets for Onboard Hydrogen Storage Systems for Light-Duty Vehicles. (U.S. Department of Energy, 2012)
- M. Carmo, D.L. Fritz, J. Mergel, D. Stolten, *Int. J. Hydrog. Energy* **38**, 4901–4934 (2013)
- C. Léger, S. Dementin, P. Bertrand, M. Rousset, B. Guigliarelli, J. Am. Chem. Soc. **126**, 12162–12172 (2004)
- G. Goldet, A.F. Wait, J.A. Cracknell, K.A. Vincent, M. Ludwig, O. Lenz, B. Friedrich, F.A. Armstrong, *J. Am. Chem. Soc.* **130**, 11106–11113 (2008)
- G. Goldet, C. Brandmayr, S.T. Stripp, T. Happe, C. Cavazza, J.C. Fontecilla-Camps, F.A. Armstrong, *J. Am. Chem. Soc.* **131**, 14979–14989 (2009)
- H.D. Hoberman, D. Rittenberg, *J. Biol. Chem.* **147**, 211–227 (1943)
- J.N. Butt, M. Filipiak, W.R. Hagen, *Eur. J. Biochem.* **245**, 116–122 (1997)
- K.A. Vincent, J.A. Cracknell, O. Lenz, I. Zebger, B. Friedrich, F.A. Armstrong, *Proc. Natl. Acad. Sci.* **102**, 16951–16954 (2005)
- A. Parkin, C. Cavazza, J.C. Fontecilla-Camps, F.A. Armstrong, *J. Am. Chem. Soc.* **128**, 16808–16815 (2006)
- K.A. Vincent, A. Parkin, F.A. Armstrong, *Chem. Rev.* **107**, 4366–4413 (2007)
- G. Goldet, A.F. Wait, J.A. Cracknell, K.A. Vincent, M. Ludwig, O. Lenz, B.r. Friedrich, F.A. Armstrong, *J. Am. Chem. Soc.* **130**, 11106–11113 (2008)
- A. Bakac, J.H. Espenson, *J. Am. Chem. Soc.* **106**, 5197–5202 (1984)
- S.C. Jackels, K. Farmery, E.K. Barefield, N.J. Rose, D.H. Busch, *Inorg. Chem.* **11**, 2893–2901 (1972)
- A. M. Tait, D. H. Busch, In: *Inorg. Synth.* ed. By B. E. Douglas (Wiley Interscience, New York, 1978) pp 22–26
- E. Uhlig, D. Schneider, *Z. Anorg. Allg. Chem.* **343**, 299–307 (1966)
- G. Costa, G. Mestroni, E. de Savognani, *Inorg. Chim. Acta* **3**, 323–328 (1969)
- K.M. Long, D.H. Busch, *J. Coord. Chem.* **4**, 113–123 (1974)
- J.L. Karn, D.H. Busch, *Nature* **211**, 160–162 (1966)
- J.L. Karn, D.H. Busch, *Inorg. Chem.* **8**, 1149–1153 (1969)
- A. M. Tait, D. H. Busch, In: *Inorg. Synth.* ed. By B. E. Douglas (Wiley Interscience, New York, 1978) pp 17–21
- L. Fabbri, A. Poggi, *Inorg. Chim. Acta* **39**, 207–210 (1980)
- V.G. Märkl, G.Y. Jin, C. Schoemer, *Tetrahedron Lett.* **21**, 1409–1412 (1980)
- L. J. Higham, M. K. Whittlesey, P. T. Wood, *Dalton Trans.*, 4202–4208 (2004)
- N.G. Connelly, W.E. Geiger, *Chem. Rev.* **96**, 877–910 (1996)
- Purwanto, R.M. Deshpande, R.V. Chaudhari, H. Delmas, *J. Chem. Eng. Data* **41**, 1414–1417 (1996)
- S. Nakagawa, A. Kudo, M. Azuma, T. Sakata, *J. Electroanal. Chem.* **308**, 339–343 (1991)
- A. Bakac, M.E. Brynildson, J.H. Espenson, *Inorg. Chem.* **25**, 4108–4114 (1986)

62. L.A.M. Baxter, A. Bobrowski, A.M. Bond, G.A. Heath, R.L. Paul, R. Mrzljak, J. Zarebski, *Anal. Chem.* **70**, 1312–1323 (1998)
63. J. Wenrui, L. Kun, *J. Electroanal. Chem.* **216**, 181–201 (1987)
64. S. Cobo, J. Heidkamp, P.-A. Jacques, J. Fize, V. Fourmond, L. Guetaz, B. Joussetme, V. Ivanova, H. Dau, S. Palacin, M. Fontecave, V. Artero, *Nat. Mater.* **11**, 802–807 (2012)
65. E. Anxolabéhère-Mallart, C. Costentin, M. Fournier, M. Robert, *J. Phys. Chem. C* **118**, 13377–13381 (2014)
66. I. Kaljurand, A. Kütt, L. Sooväli, T. Rodima, V. Mäemets, I. Leito, I.A. Koppel, *J. Org. Chem.* **70**, 1019–1028 (2005)
67. R.R. Gagne, D.M. Ingle, *J. Am. Chem. Soc.* **102**, 1444–1446 (1980)
68. R.R. Gagne, D.M. Ingle, *Inorg. Chem.* **20**, 420–425 (1981)
69. D. A. Gangi, R. R. Durand, *J. Chem. Soc., Chem. Commun.*, 697–699 (1986)
70. M.H. Schmidt, G.M. Miskelly, N.S. Lewis, *J. Am. Chem. Soc.* **112**, 3420–3426 (1990)
71. E. Fujita, C. Creutz, N. Sutin, D.J. Szalda, *J. Am. Chem. Soc.* **113**, 343–353 (1991)
72. A.D. Wilson, K. Frazee, B. Twamley, S.M. Miller, D.L. DuBois, M. Rakowski DuBois, *J. Am. Chem. Soc.* **130**, 1061–1068 (2007)
73. I. Kosuke, *Acid-base dissociation constants in dipolar aprotic solvents* (Blackwell Scientific Publications, Oxford, 1990)
74. B.J. Fisher, R. Eisenberg, *J. Am. Chem. Soc.* **102**, 7361–7363 (1980)
75. P. Du, K. Knowles, R. Eisenberg, *J. Am. Chem. Soc.* **130**, 12576–12577 (2008)
76. M. Koper, E. Bouwman, *Angew. Chem. Int. Ed.* **49**, 3723–3725 (2010)
77. J.L. Dempsey, J.R. Winkler, H.B. Gray, *J. Am. Chem. Soc.* **132**, 16774–16776 (2010)
78. E. Szajna-Fuller, A. Bakac, *Eur. J. Inorg. Chem.*, 2488–2494 (2010)